Optics Communications 340 (2015) 1–4

Contents lists available at ScienceDirect

Optics Communications

journal homepage: www.elsevier.com/locate/optcom

High sensitivity plasmonic sensing based on Fano interference in a rectangular ring waveguide

Zhao Chen [a,b,*], Luna Cui [a,b], Xiaokang Song [a,b], Li Yu [a,b], Jinghua Xiao [a,b]

[a] State Key Laboratory of Information Photonics and Optical Communications, Beijing University of Posts and Telecommunications, Beijing 100876, China
[b] School of Science, Beijing University of Posts and Telecommunications, Beijing 100876, China

ARTICLE INFO

Article history:
Received 8 August 2014
Received in revised form
20 October 2014
Accepted 25 November 2014
Available online 28 November 2014

Keywords:
Surface plasmon polaritons
Plasmonic waveguide
Fano resonance
Sensor

ABSTRACT

We investigate a plasmonic waveguide system using 2-dimension finite element method, which consists of a rectangular ring metal–insulator–metal waveguide and a baffle. Numerical simulations results show that the sharp and asymmetric Fano-line shapes can be created by the proposed structure, because of the interaction between the strong trapped resonance in the FP resonator and the weak resonance in the stub resonator. An analytic model based on the scattering matrix theory is utilized to describe and explain this phenomenon. The physical features contribute to a highly efficient plasmonic nanosensor for refractive index sensing with the sensitivity of 1300 nm/RIU and a figure of merit of 6838. This plasmonic structure with such high figure of merits may find important applications in the on-chip nanosensors.

1. Introduction

Electromagnetic waves coupled to collective oscillations of free electrons in a metal, known as surface plasmon polaritons (SPPs), has regarded as the most promising way for realization of highly integrated optical circuits, and has attracted great attentions in recent years [1,2]. A large number of devices based on SPPs have been investigated and analyzed theoretically and experimentally, such as plasmonic slot waveguides [3], all-optical switches [4], and Mach–Zehnder interferometers [5]. Among them, the metal–insulator–metal (MIM) structure has attracted more and more attention due to their deep-subwavelength confinement of light [6], and has wide applications in deep-subwavelength optical devices, such as filter [7], the absorption switches [8], Y-bend combiner [9], and plasmonic electro-optical switching [10]. As a fundamental resonant effect, the Fano resonance, which arises from the interference between a localized state and a continuum band [11], has been widely known in numerous physics systems, such as metamaterials [12], a metallic nanodisk [13], and pentamers [14]. Different from the Lorentzian resonance, the Fano resonance exhibits a typical sharp and asymmetric line profile [15], which has great important applications in demultiplexing [16], plasmonic switch [17], and so on. The specific feature of Fano resonance promises applications in sensors [18]. Thus, combining the Fano resonance with plasmonic structures would open the possibility to achieve ultracompact functional optical components in highly integrated optics [19]. The devices based on the Fano resonance show high sensitivity and a large figure of merit (FOM) due to the microscopic origin as an interference phenomenon and the unique line shapes of the Fano resonance, which can be used in sensors, lasing, switching, and nonlinear and slow-light devices.

In this paper, a rectangular ring MIM waveguide with a metal baffle is proposed and the properties of the structure are investigated numerically by the finite element method (FEM). Simulation results show that sharp and asymmetric Fano-line shape emerges in the plasmonic structure, when the baffle is put into the rectangular ring. Due to the presence of the baffle, new stub resonators are formed in the rectangular ring, and the two stub resonators with the connection waveguide are proposed as an F–P resonator. The interaction between the strong trapped resonance in the FP resonator and the weak resonance in the stub resonator gives rise to the Fano resonance. This phenomenon can be well explained by the scattering matrix theory. The proposed structure is expected to work as an excellent plasmonic sensor with a sensitivity of about 1300 nm/RIU and a FOM of about 6838.

2. Structures and simulations

The proposed plasmonic waveguide structure is schematically shown in Fig. 1(a), the sketch of the plasmonic structure is

* Corresponding author at: State Key Laboratory of Information Photonics and Optical Communications, Beijing University of Posts and Telecommunications, Beijing 100876, China.
E-mail address: bupt.yuli@gmail.com (L. Yu).

http://dx.doi.org/10.1016/j.optcom.2014.11.081
0030-4018/

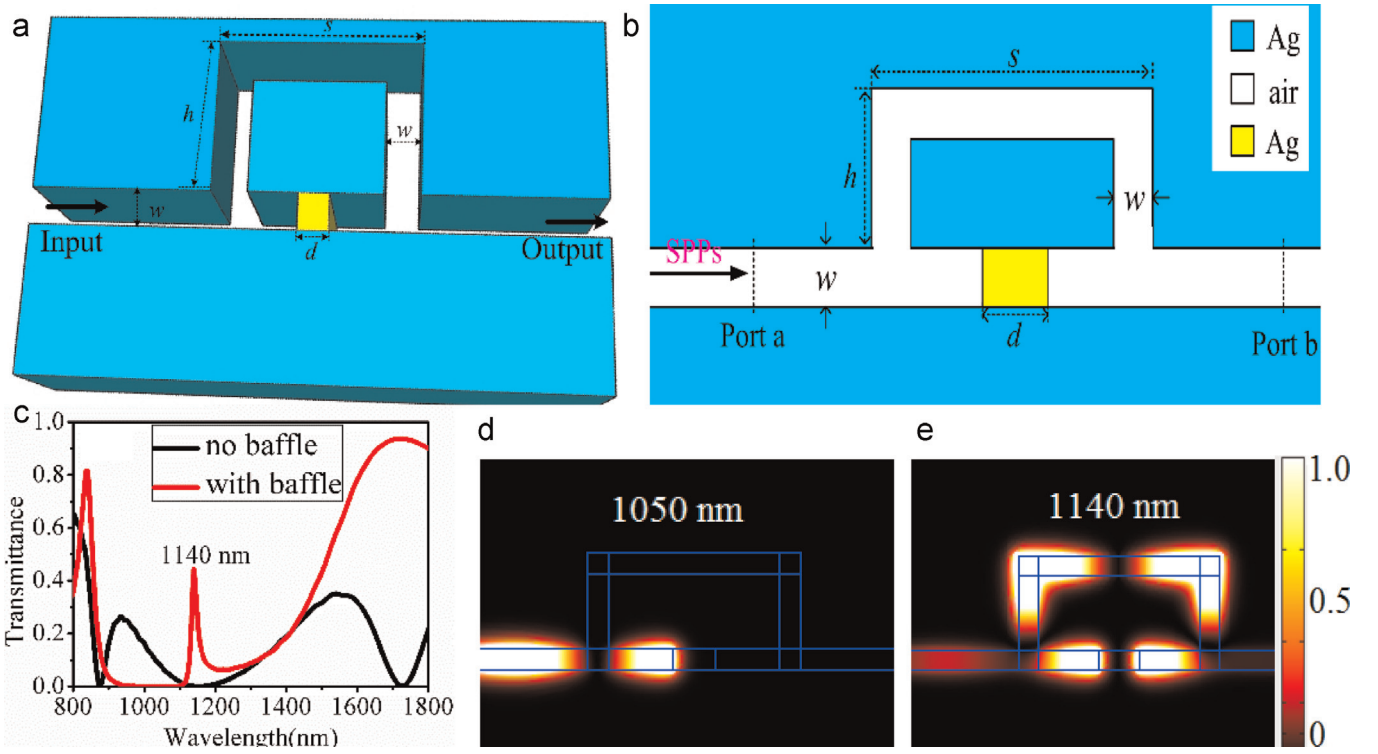

Fig. 1. Schematic of the rectangular ring MIM waveguide with a baffle and the geometrical parameter symbols: (a) 3-dimension, (b) 2-dimension. (c) Transmission spectra of port b without baffle (black curve) and with baffle (red curve), respectively. Corresponding field distributions (|Hz|) of the optical system with $d=100$ nm at the incident wavelength (d) 1050 nm, (e) 1140 nm. (For interpretation of the references to color in this figure legend, the reader is referred to the web version of this article.)

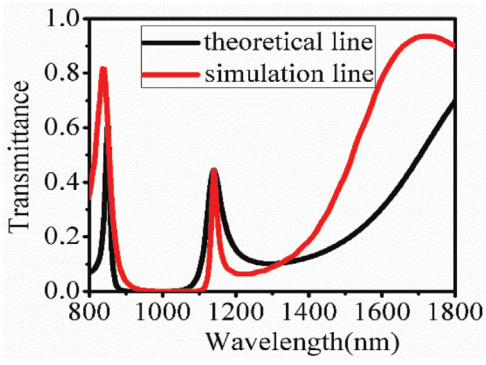

Fig. 2. Transmission spectra of analytic model result (black line) and simulation result (red line). (For interpretation of the references to color in this figure legend, the reader is referred to the web version of this article.)

composed of a rectangular ring MIM waveguide and a baffle. Fig. 1 (b) shows the 2-dimension schematic structure of Fig. 1(a). The baffle can be metals or dielectric with high refractive index. This system is a two-dimensional model, and the blue, white and yellow areas are chosen to be Ag, air and Ag, respectively. Without the baffle, the power flow of SPPs goes to port b in two directions and will interfere with each other. With the baffle, the proposed structure formed a stub resonator on each side of the baffle, the two stub resonators would affect and coupled with each other through the connection part of the MIM waveguide, which may affect the transmission spectra significantly.

The properties of Fig. 1(b) are numerically investigated using the finite element method (FEM) with Comsol Multiphysics. Since the width of the bus guide is much smaller than the wavelength of the incident light, only a single propagation mode TM_0 can exist in the structure. Therefore, when a TM-polarized plane wave is injected into the MIM structure, the incident light will be coupled

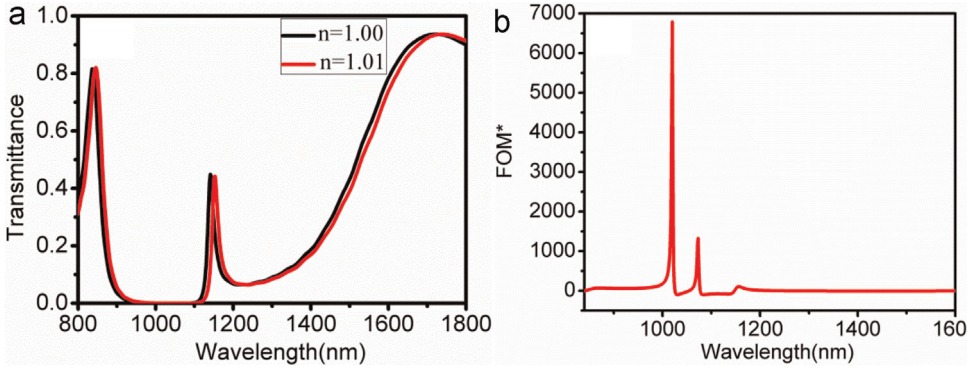

Fig. 3. (a) Transmission spectra obtained by FEM simulation for different refractive index (n). (b) Calculated FOM* at different wavelengths. (For interpretation of the references to color in this figure legend, the reader is referred to the web version of this article.)

into the bus waveguide and SPP waves are formed on the two metal interfaces. The width of the bus waveguide is w, and the length and height of the rectangular ring are s and h, respectively, d is the thickness of the baffle. The transmittance of SPPs, T, at port b is defined as the quotient between the SPPs power flows of port b and port a. The power flows at the ports are obtained by integrating the Poynting vector over the channel cross section. In the simulation, the permittivity of Ag can be determined by the well-known Drude model: $\varepsilon_m=\varepsilon_\infty-\omega_p^2/(\omega^2+i\omega\gamma)$ with $\varepsilon_\infty=3.7$, $\omega_p=9.1$ eV, $\gamma=0.018$ eV, [20], which fits the experimental optical constant of silver [21] for the range of 600 nm–2000 nm quite well. We investigate the properties of the proposed structure in frequency domain, in the simulation, the MIM dielectric gap, and the rectangular ring height and length are assumed to be $w=50$ nm, $h=225$ nm, $s=500$ nm, respectively. To display the difference, the transmission spectra of the plasmonic waveguide with ($d=100$ nm) and without ($d=0$ nm) the baffle are simulated, and the results are shown by the red and black curves in Fig. 1(c), respectively. Additional simulations results (not shown in this paper) indicate that the position and size of the baffle almost has no influence on the transmission profile. For simplicity, we locate the position of the baffle in the center of the rectangular ring. In addition, taking into account both the size of the structure and the skin depth of SPP in the metal (about 10–40 nm), we choose $d=100$ nm as an example.

Clearly, it is observed that the transmission spectra (black curve) become sharp and asymmetric (red curve) when the thickness of the baffle is $d=100$ nm, which is quite different from that $d=0$ nm (no baffle). For the asymmetric spectra, the transmittance of the SPPs varies sharply from the valley to the peak with small wavelength shift of about $\Delta\lambda=35$ nm. The corresponding field distributions at the valley and peak positions for $d=100$ nm are displayed in Fig. 1(d) and (e), respectively. At $\lambda=1050$ nm, the SPPs are blocked by the new stub resonator, and almost no SPPs transport to the output. At $\lambda=1140$ nm, strong field distributions are obviously observed between the two new stub resonators. Due to the presence of the baffle, two new stub resonators emerge, and part SPPs can be reflected back and forth between them, which is just like an FP resonator. In addition, the other two resonance peaks also support the FP model. The accumulated phase delay per round trip is $\varphi_{FP}=4\pi n_{eff}L/\lambda+\theta$, here n_{eff} is the effective index of SPPs in the MIM waveguide, L is the distance that SPPs propagates from one stub resonator to another, which is denoted as $L=2(s+h-w)-d$ and θ is the phase shifts brought by the reflection in the FP resonator. From Fig. 1(e), we can see that a strong trapped resonance occurs in the FP resonator, resulting in a narrow transmission peak. The sharp and asymmetric spectra, usually termed as Fano profiles, result from the coupling of a narrow discrete resonance (strong trapped resonance in the FP resonator) and a broad spectrum (stub resonator) [11,15].

3. Analyze model

To analyze the behavior of this phenomenon above, we use the scattering matrix theory [22,23] to illustrate the transmission spectra in the proposed system. Quantitatively, the scattering property of the single stub resonator for the incident waves at a frequency ω can be described using a transfer matrix T_t, which relates to the incoming and outgoing SPPs amplitudes at port a (a_1 and b_1) to port b (a_2 and b_2):

$$\begin{bmatrix} b_2 \\ a_2 \end{bmatrix} = T_t \times \begin{bmatrix} a_1 \\ b_1 \end{bmatrix} = \begin{bmatrix} 1-\dfrac{i\gamma_0}{\omega-\omega_0} & \dfrac{-i\gamma_0}{\omega-\omega_0} \\ \dfrac{i\gamma_0}{\omega-\omega_0} & 1+\dfrac{i\gamma_0}{\omega-\omega_0} \end{bmatrix} \times \begin{bmatrix} a_1 \\ b_1 \end{bmatrix} \quad (1)$$

where $\omega_0=c/\lambda_0$ and $\gamma_0=(1/2)\Delta\lambda_{FWHM}/\lambda_0^2$ are the center frequency and the width of the resonance, ω is the angular frequency of the incident light. For the phase shift coming from the stub resonator to the other stub resonator has the form of [23]:

$$T_p = \begin{bmatrix} \exp(i\varphi_{FP}) & 0 \\ 0 & \exp(-i\varphi_{FP}) \end{bmatrix} \quad (2)$$

Therefore, the transfer matrix T_{all} for Fig. 1(a) can be expressed as the following equation:

$$T_{all} = T_t \times T_p \times T_t \quad (3)$$

From the Eqs. (1), (2) and (3), we can get the amplitude transmittance t_s in the system to be $t_s=1/T_{all,22}$, the transmitted intensity of this system is determined by $|t_s|^2$. To demonstrate the phenomenon and the validity of the equations above, we have carried out the intensity transmission spectrum by in Eq. (3). Fig. 2 shows the calculated transmission spectra (black line) and the simulation line (red line). It is easy to know that the analytical results and the FEM simulation results match each other very well. Here, the slight deviation from the simulation result is due to the intrinsic loss of the structure and the propagation loss.

4. Sensing applications based on Fano resonance

By utilizing the asymmetric Fano transmission spectrum, we study the performance of our structure as a plasmonic nanosensor, and the results are displayed in Fig. 3(a). It is observed that the Fano line-shapes has a red shift of about 13 nm when the refractive index of the connection waveguide changes from $n=1.00$ to $n=1.01$, as shown by the black and red lines in Fig. 3(a). The sensitivity of a sensor (nm/RIU) is usually defined as the shift in the resonance wavelength per unit variations of the refractive index [24]. The sensitivity of the proposed structure is about 1300 nm/RIU, which is excellent compared with that of the plasmonic sensors reports [24,25]. For better quantification, the plasmonic sensor detects the relative intensity change $dI(\lambda)/dn(\lambda)$ at a fixed wavelength λ_0. An FOM, which is introduced by Becker et al., is defined as $FOM^*=\max|dI(\lambda)/Idn(\lambda)|$ [26], where $dI(\lambda)/dn(\lambda)$ is the relative intensity change at a fixed wavelength induced by a refractive index change dn. $I(\lambda_0)$ corresponds to the intensity when the FOM* reaches a maximum value. Fig. 3(b) depicts the calculated FOM*. The maximum value of the FOM* is as high as 6838 at $\lambda=1020$ nm, which is due to the sharp asymmetric Fano line-shape with ultra-low transmittance at this wavelength. The FOM* is much higher than that of the plasmonic sensors in [24,25]. Moreover, it is noted that the FOM* is greater than 1000 at $\lambda=1070$ nm.

5. Conclusion

In summary, a rectangular ring MIM waveguide with a baffle is proposed and investigated by FEM. Simulation results show that sharp and asymmetric Fano-line shape emerges in the plasmonic structure, when the baffle is put into the rectangular ring. Due to the presence of the baffle, new stub resonators are formed in the rectangular ring, and the two stub resonators with the connection waveguide are proposed as an F–P resonator. The interaction

between the strong trapped resonance in the FP resonator and the weak resonance in the stub resonator gives rise to the Fano resonance. An analytic model based on scattering theory is provided to explain this phenomenon, which matches the FEM simulation results quite well. At last, we use the sharp and asymmetric Fano line-shape to achieve a highly sensitive plasmonic nanosensor with the sensitivity of 1300 nm/RIU and FOM* of 6838. The mechanism based on Fano resonance may provide a novel method for designing high sensitivity plasmonic components in optical communication.

Acknowledgments

This work was supported by the National Natural Science Foundation of China under Grant no. 11374041, National Basic Research Program of China under Grant no. 2010CB923202 and Fund of State Key Laboratory of Information Photonics and Optical Communications (Beijing University of Posts and Telecommunications), PR China.

References

[1] W.L. Barnes, A. Dereux, T.W. Ebbesen, Nature 424 (2003) 824.
[2] R. Zia, J.A. Schuller, A. Chandran, M.L. Brongerma, Mater. Today 9 (2006) 20.
[3] J.A. Dionne, L.A. Sweatlock, H.A. Atwater, Phys. Rev. B 73 (2006) 035407.
[4] G.A. Wurtz, R. Pollard, A.V. Zayats, Phys. Rev. Lett. 97 (2006) 057402.
[5] B. Wang, G.P. Wang, Opt. Lett. 29 (2004) 1992.
[6] I.D. Leon, P. Berini, Nat. Photon. 4 (2010) 382.
[7] X.S. Lin, X.G. Huang, Opt. Lett. 33 (2008) 2874.
[8] A.R. Davoyan, I.V. Shadrivov, A.A. Zharov, D.K. Gramotnev, Y.S. Kivshar, Phys. Rev. Lett. 105 (2010) 116804.
[9] A. Noual, A. Akjouj, Y. Pennec, J.-N. Gillet, B. Djafari-Rouhani, N. J. Phys. 11 (2009) 103020.
[10] J.H. Zhu, X.G. Huang, X. Mei, Plasmonics 6 (2011) 605.
[11] U. Fano, Phys. Rev. 124 (1961) 1866.
[12] V. Fedotov, N. Papasimakis, E. Plum, A. Bitzer, M. Walther, P. Kuo, D.P. Tsai, N.I. Zheludev, Phys. Rev. Lett. 104 (2010) 223901.
[13] Z.Y. Fang, J.Y. Cai, Z.B. Yan, P. Nordlander, N.J. halas, X. Zhu, Nano Lett. 11 (2011) 4475.
[14] G. D' Aguanno, D. de Ceglia, N. Mattiucci, M.J. Bloemer, Opt. Lett. 36 (2011) 1984.
[15] A. Miroshnichenko, S. Flach, Y. Kivshar, Rev. Mod. Phys. 82 (2010) 2257.
[16] J.J. Chen, Z. Li, J. Li, Q.H. Gong, Opt. Express 19 (2011) 9976.
[17] W.S. Chang, J.B. Lassiter, P. Swanglap, H. Sobhani, S. Khatua, P. Nordlander, N.J. Halas, S. Link, Nano Lett. 12 (2012) 4977.
[18] B. Luk' yanchuk, N. Zheludev, S. Maier, N. Halas, P. Nordlander, H. Giessen, C. Chong, Nat. Mater. 9 (2011) 707.
[19] N. Liu, L. Langguth, T. Weiss, J. Kastel, M. Fleisch, T. Pfau, H. Giedden, Nat. Mater. 8 (2009) 758.
[20] T.B. Wang, X.W. Wen, C.P. Yin, H.Z. Wang, Opt. Express 17 (2009) 24096.
[21] P.B. Johnson, R.W. Christy, Phys. Rev. B 6 (1972) 4370.
[22] S.H. Fan, Appl. Phys. Lett. 80 (2002) 908.
[23] H.A. Haus, Waves and Fields in Optoelectronics, Prentice-Hall, New York, 1984.
[24] N. Liu, M. Mesch, T. Weiss, M. Hentchel, H. Giessen, Nano Lett. 10 (2010) 2342.
[25] H. Lu, X.M. Liu, D. Mao, G.X. Wang, Opt. Lett. 37 (2012) 3780.
[26] J. Becker, A. Trugler, A. Jakab, U. Hohenester, C. Sonnichsen, Plasmonics 5 (2010) 161.